Journal of Instrumentation

A multi-wirescanner test setup utilizing characteristic X-rays for charged particle and photon beam diagnostics

Jinst

Published by IOP Publishing for Sissa Medialab

Received: *September 4, 2018*
Revised: *November 14, 2018*
Accepted: *November 14, 2018*
Published: *December 7, 2018*

A multi-wirescanner test setup utilizing characteristic X-rays for charged particle and photon beam diagnostics

R.M. Nazhmudinov,[a,b,1] **A.S. Kubankin,**[a,b] **P.V. Karataev,**[c] **I.A. Kishin,**[a,b] **A.V. Vukolov,**[d] **A.P. Potylitsyn,**[d] **P.N. Zhukova**[a] **and V.A. Nasonova**[a]

[a] *Belgorod National Research University, 85, Pobedy St., Belgorod, 308015, Russian Federation*
[b] *P.N. Lebedev Physical Institute of the Russian Academy of Sciences, 53, Leninskiy Prospekt, Moscow, 119991, Russian Federation*
[c] *John Adams Institute at Royal Holloway, University of London, Egham, Surrey, TW20 0EX, United Kingdom*
[d] *National Research Tomsk Polytechnic University, 30, pr. Lenina, Tomsk, 634050, Russian Federation,*

E-mail: nazhmudinov@bsu.edu.ru

Abstract: A multi-wirescanner for diagnostics of ionizing particle beams (e.g. both non-relativistic and ultra-relativistic charged particles; X-ray and gamma photons) is proposed and discussed in the paper. The scanner is based on measurement of yield of characteristic X-rays generated during the particle interaction with the wires made of different materials. The proposed scanner is developed and tested on the beam of electrons with energy of 40 keV. The quasimonochromatic characteristic X-rays and continuous background are clearly identified. The results of measurements of the transverse size, emittance, position and direction of beam propagation are presented and discussed.

Keywords: Beam-line instrumentation (beam position and profile monitors; beam-intensity monitors; bunch length monitors); Instrumentation for particle accelerators and storage rings - high energy (linear accelerators, synchrotrons); Instrumentation for particle accelerators and storage rings - low energy (linear accelerators, cyclotrons, electrostatic accelerators)

[1]Corresponding author.

https://doi.org/10.1088/1748-0221/13/12/P12012

2018 JINST 13 P12012

Contents

2018 JINST 13 P12012

1 Introduction

Diagnostics equipment is an important element of any accelerator. There are a huge number of devices working on different physical principles and designed to measure such parameters of charged particle beams as transverse and longitudinal size, angular divergence, emittance, position, trajectory, arrival time, energy spread, etc. [1–3]. These sensors represent a diagnostics family capable of visualizing the particle beam behavior in an accelerator aiding its operation, optimization and manipulation.

Beam size measurement is crucial to evaluate the performance of an accelerator facility. In circular machines synchrotron radiation, appearing when a charged particles is bent in a dipole magnet, is utilized [4–6]. However, in linear accelerators one needs to introduce a mechanism of interaction with the particle beam that reveals its parameters. Scintillator screen monitors were initially introduced [7]; however, due to limited resolution and quick saturation by a high power beam, they were replaced by optical transition radiation (OTR) screens [8]. OTR screen monitors provided 2D beam profile measurements reaching micron-scale resolution [9], however, due to emission of coherent light these monitors malfunction at very short bunches of X-ray free electron lasers [10]. Furthermore, at non-relativistic energies the OTR intensity is rather low.

The state-of-the-art in transverse beam size and emittance diagnostics is the so-called laser-wire. In this case a thin laser beam is scanned across a particle beam. The secondary particles (e.g. backscattered gamma-photons [11] or photo-detached electrons or neutral hydrogen atoms from H^- particles [12]) are detected downstream. This is a rather complicated system requiring an expensive laser, sophisticated laser beam transport line, and a team of people to operate.

Solid wire scanners were also introduced in a very early period of accelerator development. Due to simplicity of construction, high-enough resolution and relatively low cost wire scanners are still used to measure transverse position, direction, profile, emittance, and energy spread of the particle beams. The wire scanners are used for beam monitoring at low [13–15], medium [16–18] and high energies [19, 20], as well as in sources of photons [21]. During the measurement, the wire is scanned across the particle beam, while the electrical current induced by the beam [22] or

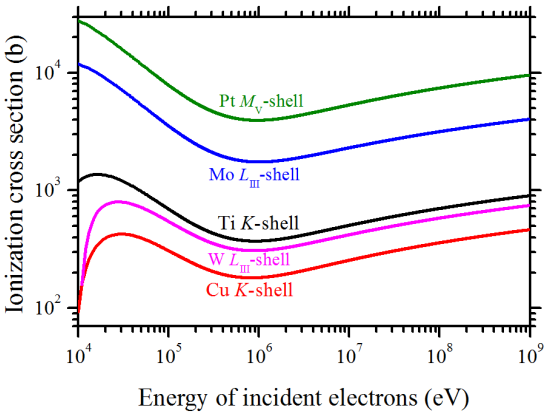

Figure 1. Example of cross sections for ionization K, L and M shells of different atoms by electron impact.

the intensity of the secondary particles [23] are registered. In long linear accelerators the detector has to be placed at a very large distance from the interaction region. Moreover, it also picks up background photons generated by the beam halo particles co-propagating with the beam.

In this paper we present a modification of the wire scanner, which makes it possible to measure the trajectory, dimensions and emittance of a particle beam at an arbitrary location of the detector using the characteristic X-ray radiation generated by the beam in a set of wires made of different materials. It enables to distinguish signals from different wires and subtract background from the same measurement.

2 Characteristic X-ray emission

Characteristic X-rays (CXR) are generated during relaxation of an atom ionized by either a fast charged particle or an energetic X-ray or gamma photon. The atoms of different elements emit unique spectra of characteristic X-ray lines. The characteristic radiation of an atom has isotropic distribution for different particles and energies. If the wires are made of different materials then the measured spectra allow to separate the signal from the wires. It is evident that the intensity of the signal at each step of the wire is proportional to the number of particles directly interacting with the wire. It is an important detail that the X-ray detector can be placed under different observation angles relative to the direction of the particles propagation in contrast with the scanners based on detection of bremsstrahlung propagating at a small angle (typical angles are less than γ^{-1}, where γ is the Lorenz-factor of a charged particle) relative to the particle direction. This detail is convenient in an experiment because the detector can be placed in the area where background has the lowest level.

Figure 1 shows the calculation of the ionization cross-sections of atomic shells (we used in an experiment) by fast electrons with energies from 10 keV to 1 GeV [24]. It is a great advantage that in such a wide range of energies of incident particles the ionization cross section changes by no more than an order of magnitude for each shell. This feature makes it possible to use CXR to monitor the particle beam parameters at both low and high energies.

2018 JINST 13 P12012

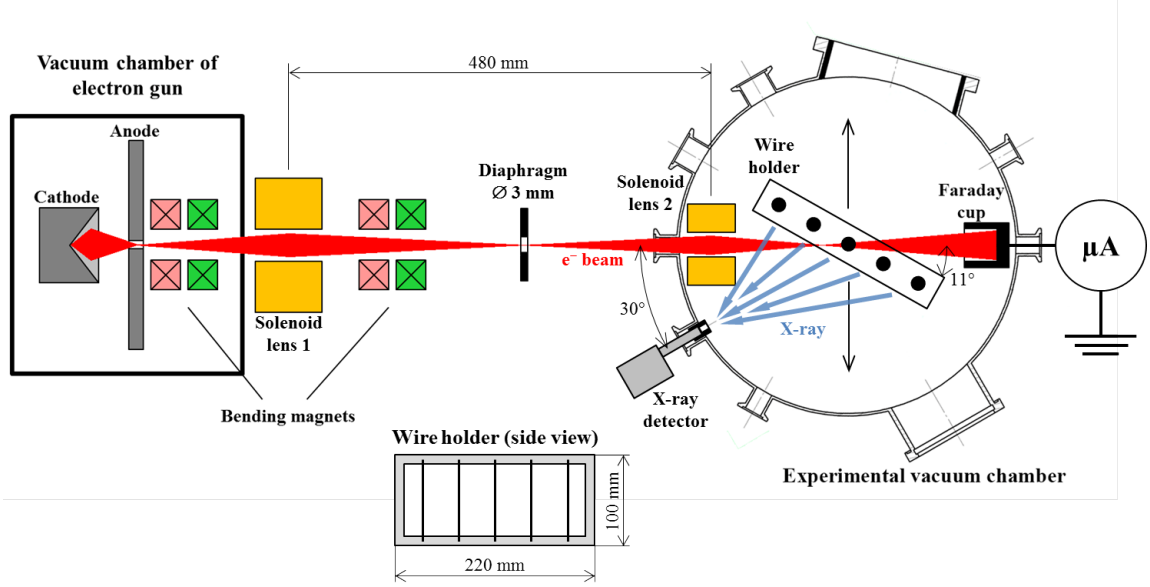

Figure 2. The experimental station: DC beam is produced by the electron gun, formed by two solenoid lenses and transported to the experimental vacuum chamber; the wires in the holder can simultaneously move across the beam axis as shown by the black arrows; the spectra of CXR photons are registered by the X-ray detector.

3 Experimental setup

An experimental station for investigation of various mechanisms of EM radiation generation by a continuous electron beam was designed and manufactured at Radiation Physics Laboratory of Belgorod National Research University [25]. The scheme of an experimental setup is presented in figure 2.

The setup consists of the DC electron gun, beam transport system, vacuum chamber with the wire scanner and equipment for measurement of X-ray spectra and electron beam current. The DC electron gun with thermionic tungsten filament produces an electron beam with energy in the range from 10–100 keV and beam current of up to 500 μA. The beam transport system includes two solenoid lenses and two pairs of dipole correctors. In the focal point of the 1st lens a metal diaphragm with an aperture diameter of 3 mm is mounted. The 2nd lens is located inside the experimental vacuum chamber. The vacuum chamber has an internal diameter of 400 mm. The second lens enables us to adjust the position of the beam waist at the wire assembly for emittance measurement. A Faraday cup and microammeter are used to measure the beam current. A scintillator screen at the end of the beam trajectory is used to observe the beam position.

The scanner consists of five wires of different materials mounted on a holder, which is an aluminum frame of 220 × 100 mm^2. To avoid the overlapping of the wires, the holder plane is positioned at an angle of 11° to the axis of the electron beam channel. During the beam scan the holder moves in horizontal direction perpendicular to the beam axis. The wires scan across the electron beam at different points along the beam axis. When particles of the beam interact with the wires, bremsstrahlung and characteristic X-rays are generated with intensity depending on the transverse position of the wire with respect to the electron beam centroid [26]. At this

2018 JINST 13 P12012

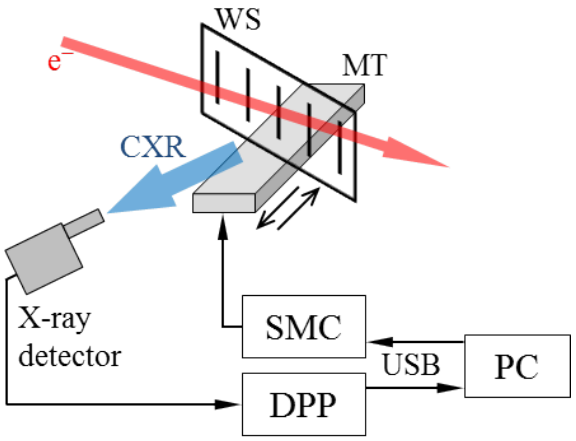

Figure 3. Schematic diagram for beam parameter measurements.

energy of electrons both CXR and bremsstrahlung mechanisms produce radiation with isotropic angular distribution. However, bremsstrahlung has a continuous spectrum which does not allow separating the signal from different wires and the background. Moreover, in case of relativistic beams, bremsstrahlung is directed along the particle trajectory within an open angle of order of $1/\gamma$. Due to isotropic angular distribution at high energies CXR is even more promising because of monochromatic spectrum that depends on the wire material [27]. A possibility to measure the CXR spectra by a semiconductor detector under the influence of the radiation background was demonstrated for different particle beams [28, 29].

The schematic diagram for measuring the beam parameters by wire scanner (WS) is shown in figure 3. To separate signals we used the following wires: 45-μm titanium wire, 100-μm tungsten wire, 100-μm molybdenum wire, 85-μm copper wire and 95-μm thick platinum wire. A silicon drift X-ray detector Amptek XR100SDD FAST with 12.5 μm thick beryllium window and 500 μm thick silicon crystal was used to measure the radiation spectra. The effective area of the input detector window was 17 mm^2. Measured energy resolution of the detector at 5.9 keV was about 170 eV. The efficiency in the energy range form 1–25 keV was more than 20%.

The detector signal is processed in the digital pulse processor (DPP) Amptek PX5 controlled by a PC. The position of the scanner is controlled by a motorized linear translation stage (MT) Standa 8MT175-100-VSS42 and a stepper motor controller (SMC) Standa 8SMC1-USBhF-B2-4 with accuracy of about 2.5 μm. To control the wire scanner, we created the software in the LabVIEW integrated development environment.

4 Results and discussion

This section presents experimental results obtained for electrons with energy of 40 keV and beam current of 1 μA. Low current was chosen to avoid the detector saturation and the thermal damage of the wires after long exposure. Nevertheless short test has demonstrated that the beam size does not change when increasing the beam current. That is because the charge density of our DC beam is not high enough to trigger the space charge effect. Figure 4 shows an example of X-ray spectra

2018 JINST 13 P12012

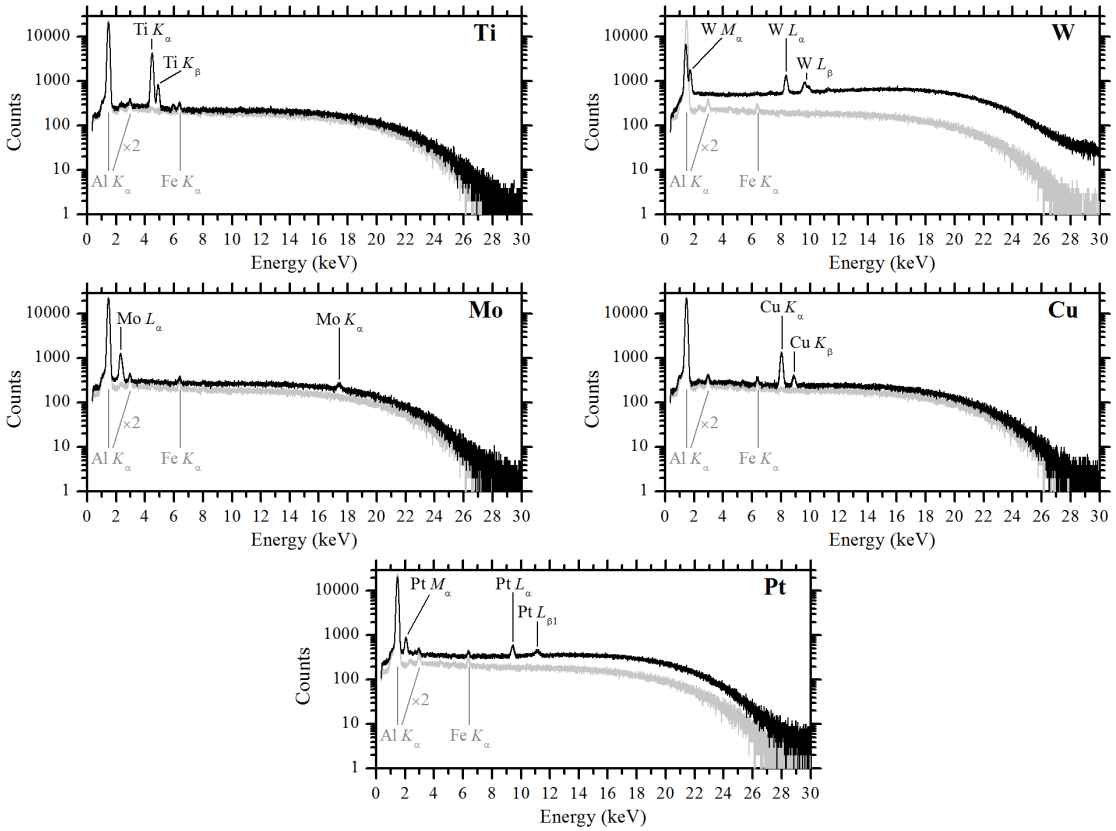

Figure 4. X-ray spectra of the wires (black line) and background (gray line).

produced in the wires made of different materials. The peaking time of the spectroscopic system is 0.4 µs. The acquisition time is chosen to get clear spectra. However, as it is shown later, even at this low beam current the acquisition time can be reduced down to a few seconds to shorten the beam profile measurement duration. To avoid overloads, a lead collimator with aperture diameter of 1.7 mm was installed in front of the detector window (the average solid angle is about 6×10^{-5} sr).

It can be seen that the spectra contain CXR, radiation from the holder (aluminum) and the vacuum chamber (iron) materials, as well as the continuous bremsstrahlung contribution from the wire itself. The background spectrum is obtained with the wires removed from the beam. One may see the background generated upstream or downstream the wire assembly is significantly smaller than the bremsstrahlung contribution from the wire itself. However, if this methodology is applied at relativistic energies the bremsstrahlung contribution can be significantly smaller. The contribution at large observation angles will be negligible, which will certainly improve the signal-to-noise ratio. On the other hand the background from the beam can be much larger. Therefore a separate experimental test at high energies is needed.

To obtain the transverse profile of the beam it is required to measure the dependence of the CXR intensity of a particular wire (K_α for titanium and copper, L_α for molybdenum and tungsten, and M_α for platinum) on the position of the scanner. It is necessary to exclude the contribution of background to improve the signal to noise ratio. The CXR photon yield strongly depends on the wire materials. However, the continuous pedestal in figure 5 contains both bremsstrahlung

2018 JINST 13 P12012

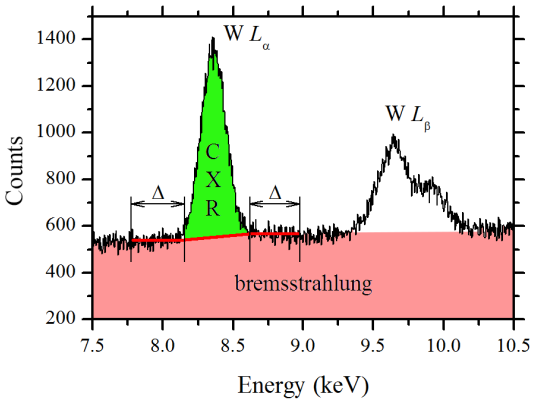

Figure 5. Example of background subtraction for tungsten L_α-line.

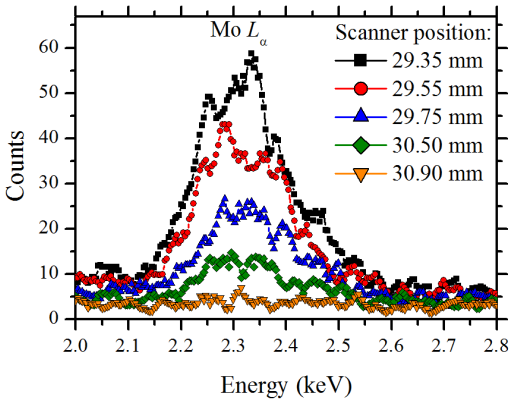

Figure 6. Molybdenum X-ray spectrum change during scanning.

and background photons. We assume that the pedestal under the CXR peak varies linearly in the vicinity of the mean values in the border areas Δ as shown in figure 5, and, therefore, can be subtracted. This procedure simplifies the calculation of the peak area and is suitable for quick automatic measurements. Figure 6 shows how the X-ray spectrum of molybdenum wire changes during the scan. The acquisition time for each spectrum is about 1 s, which is enough to collect proper statistics. One may see that the continuous level also depends on the wire position. However, subtracting it from the main signal we isolate CXR photons, to obtain clear beam profiles.

The results of measurements of the beam profiles are shown in figure 7. The measurements are performed in steps of 50 µm and exposure time of 1 s for each point on the graphs. The total scan time was about 1 hour, but each wire was exposed to the electron beam for 3 minutes. Therefore the total scan time can be reduced down to 20 minutes optimizing the scan methodology. Moreover, the maximum number of events in the measured profiles allows to further reduce the scan time by a factor of 10.

It is clear that the electron beam is not Gaussian, but consists of the main part (the core) and a satellite part. In order to extract the beam dimensions from the measured profiles, a sum of two Gaussian functions (one for the core and one for the satellite) was used to fit the experimental data:

$$N_{\mathrm{CXR}}(x) = N_0 + \frac{A_1}{\sqrt{2\pi}\sigma_1} e^{-\frac{(x-x_1)^2}{2\sigma_1^2}} + \frac{A_2}{\sqrt{2\pi}\sigma_2} e^{-\frac{(x-x_2)^2}{2\sigma_2^2}}, \tag{4.1}$$

where N_{CXR} is the number of photons in CXR peak, N_0 is the offset, A_1 and A_2 are the areas, and x_1 and x_2 are the positions of the core and the satellite respectively, σ_1 and σ_2 are the widths of the core and satellite peaks, x is the position of the scanner. The fitting parameters for each profile and the corresponding coefficients of determination (R^2) are summarized in table 1.

Figure 8 shows how the size of the beam core σ_1 varies along its axis. The minimum size of the beam core $\sigma_{\mathrm{min}} = 0.148 \pm 0.013$ mm is reached at the location of the tungsten wire. Also, from the data in figure 8, we can extract values of the beam divergence of $0.46° \pm 0.06°$ and normalized emittance $\varepsilon_n = \varepsilon\beta\gamma = 0.22 \pm 0.03\,\pi$ mm mrad (where β is the speed of particle in units of the speed of light and ε is the physical beam emittance). In addition, the results of measurements make

2018 JINST 13 P12012

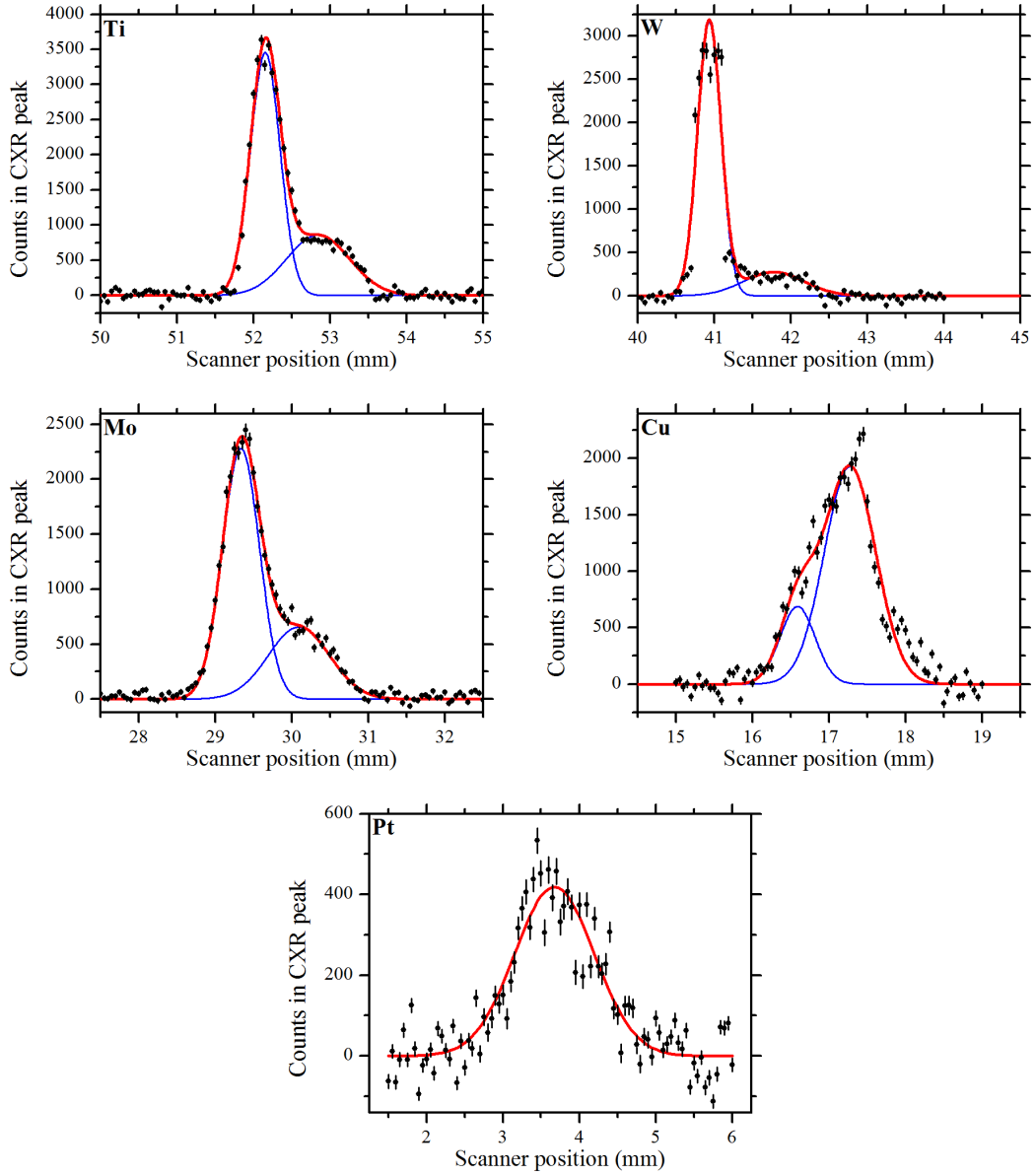

Figure 7. Measured profiles of the electron beam (points) and result of fitting by Gaussian function (lines).

Table 1. Fitting parameters for beam profiles.

		Core			Satellite			
Wire	N_0	A_1 (mm)	x_1 (mm)	σ_1 (mm)	A_2 (mm)	x_2 (mm)	σ_2 (mm)	R^2
Ti	–16±15	1686±85	52.154±0.005	0.195±0.006	885±103	52.85±0.05	0.41±0.06	0.987
W	–32±36	1209±65	40.935±0.007	0.153±0.008	271±114	41.78±0.14	0.40±0.17	0.931
Mo	22±7	1382±46	29.336±0.006	0.242±0.005	658±52	30.10±0.03	0.40±0.03	0.994
Cu	25±24	1628±141	17.277±0.031	0.337±0.026	398±128	16.59±0.06	0.23±0.05	0.953
Pt	0±10	547±37	3.675±0.026	0.614±0.037	—	—	—	0.846

2018 JINST 13 P12012

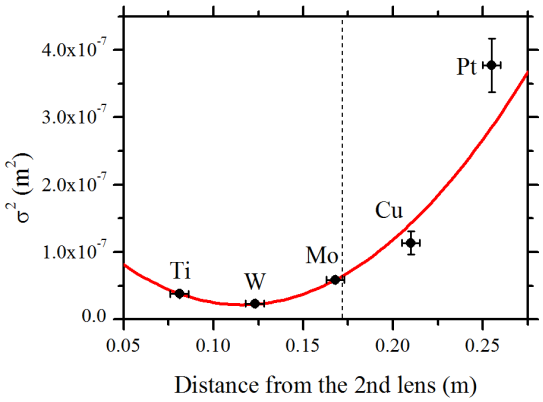

Figure 8. Measured transverse beam size of the beam core as function of distance along the beam axis (points) and parabola fitting (line); dashed line-axis of the experimental chamber.

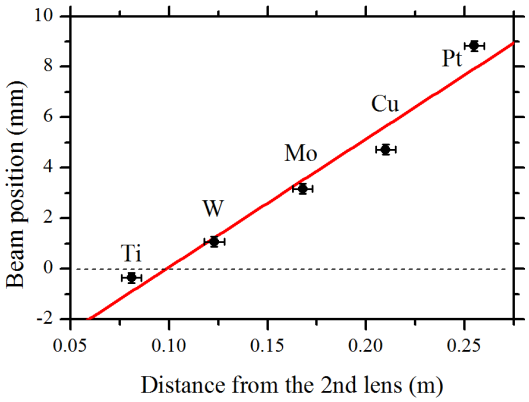

Figure 9. Measured beam position in the experimental vacuum chamber (points) and linear fitting (line); dashed line-axis of the electron beam channel.

it possible to determine the real trajectory of electrons in the experimental chamber, as shown in figure 9. The curved path comes from the fact that the beam profile changes while propagating through the chamber. The analysis has been performed for the beam core only. One may see that the emittance is by a factor of 4 smaller than previously reported in [25]. The reason is that previously were unable to separate the core from the satellite beam.

5 Conclusion

In the article, we propose a modified version of a wire scanner based on measurements of CXR spectra generated by fast particles in solid wires. The proposed wire scanner differs from the conventional one by the fact that the wires are made from different materials (or wires coated by different materials) and an energy dispersive semiconductor detector for measuring X-ray spectra. This scanner allows quick subsequent measurements of the transverse profiles of the particle beam at different longitudinal positions. Since the CXR energy depends on the material of the wire, the signals from different wires are not overlapped and can be easily separated. At these energies simultaneous measurements are not possible because all electrons interacting with wires are absorbed. At relativistic energies it might be possible. Since CXR has an isotropic angular distribution, there are no restrictions on the location of the X-ray detector, e.g. the measurements can be done in backward direction minimizing the background contribution and making the entire scanner compact and self-sufficient. The scanning time depends on the detector performance and the beam intensity. In the case of high beam currents, the CXR intensity can be reduced using collimators and (or) attenuators. The proposed wire scanner can be used to measure the main characteristics (position, divergence, size, emittance, direction) of beams of charged or neutral particles (e.g. X-ray or gamma photons) at both low and high energies. The measurements can be carried out both in vacuum and at atmospheric pressure.

2018 JINST 13 P12012

Acknowledgments

The work was financially supported by the grant of the President of Russia for young doctors of sciences MD-5748.2018.2 and by a Program of the Ministry of Education and Science of the Russian Federation for higher education establishments (project No.3.1631.2017/4.6).

References

[1] M.G. Minty and F. Zimmermann, *Measurement and control of charged particle beams*, Springer-Verlag, Berlin, Germany, (2003).

[2] P. Strehl, *Beam instrumentation and diagnostics*, Springer-Verlag, Berlin, Germany, (2006).

[3] V. Smaluk, *Particle beam diagnostics for accelerators: Instruments and methods*, VDM Verlag Dr. Müller, (2009).

[4] S. Takano, M. Masaki and H. Ohkuma, *X-ray imaging of a small electron beam in a low-emittance synchrotron light source*, *Nucl. Instrum. Meth.* **A 556** (2006) 357.

[5] M. Kocsis and A. Snigirev, *Imaging using synchrotron radiation*, *Nucl. Instrum. Meth.* **A 525** (2004) 79.

[6] K. Iida et al., *Measurement of an electron-beam size with a beam profile monitor using Fresnel zone plates*, *Nucl. Instrum. Meth.* **A 506** (2003) 41.

[7] W.S. Graves, E.D. Johnson and S. Ulc, *A high resolution electron beam profile monitor and its applications*, *AIP Conf. Proc.* **451** (1998) 206.

[8] K. Honkavaara et al., *Design of OTR beam profile monitors for the TESLA Test Facility, Phase 2 (TTF2)*, Proceedings of the *2003 Particle Accelerator Conference* **4** (2003) 2476.

[9] M. Ross et al., *A very high resolution optical transition radiation beam profile monitor*, *AIP Conf. Proc.* **648** (2003) 237.

[10] G. Kube, *Radiation sources and their application for beam profile diagnostics*, Proceedings of *IBIC-2014*, Monterey, California, U.S.A., September 14–18, 2014, http://accelconf.web.cern.ch/AccelConf/IBIC2014/papers/tuizb1.pdf.

[11] L.J. Nevay et al., *Laserwire at the Accelerator Test Facility 2 with Sub-Micrometre Resolution*, *Phys. Rev. ST Accel. Beams* **17** (2014) 072802 [arXiv:1404.0294].

[12] T. Hofmann et al., *Demonstration of a laserwire emittance scanner for hydrogen ion beams at CERN*, *Phys. Rev. ST Accel. Beams* **18** (2015) 122801 [arXiv:1508.05750].

[13] Y. Nengjie, T. Chuanxiang, Z. Shuxin, L. Quanfeng and G. Ke, *2-D low energy electron beam profile measurement based on computer tomography algorithm with multi-wire scanner*, Proceedings of the *2005 Particle Accelerator Conference*, MKnoxville, TN, U.S.A., May 16–20, 2005, pp. 4323–4325.

[14] J.F. O'Hara, J.D. Gilpatrick, L.A. Day, J.H. Kamperschroer and D.W. Madsen, *Slow wire scanner beam profile measurement for LEDA*, *AIP Conf. Proc.* **546** (2000) 510.

[15] P. Ausset et al., *Beam diagnostics instrumentation for the high energy beam transfer line of I.P.H.I.*, Proceedings of *DIPAC-2005*, Lyon, France, June 6–8, 2005, https://accelconf.web.cern.ch/AccelConf/d05/PAPERS/POT013.PDF.

[16] A.B. El-Sisi, *Wire scanner beam profile measurement for ESRF*, Proceedings of *DIPAC-2003*, Mainz, Germany, May 5–7, 2003, http://accelconf.web.cern.ch/Accelconf/d03/papers/PM16.pdf.

2018 JINST 13 P12012

[17] M.R. Hadmack and E.B. Szarmes, *Scanning wire beam position monitor for alignment of a high brightness inverse-Compton X-ray source*, Proceedings of *IBIC-2013*, Oxford, U.K., September 16–19, 2013, http://accelconf.web.cern.ch/AccelConf/ibic2013/papers/wepf21.pdf.

[18] S. Burger, C. Carli, M. Ludwig, K. Priestnall and U. Raich, *The PS booster fast wire scanner*, Proceedings of DIPAC-2003, Mainz, Germany, May 5–7, 2003, http://accelconf.web.cern.ch/AccelConf/d03/papers/PM13.pdf.

[19] M.C. Ross, J.T. Seeman, E. Bong, L. Hendrickson, D. McComiick and L. Sanchez-Chopitea, *Wire scanners for beam size and emittance measurements at the SLC*, Conference Record of the *1991 IEEE Particle Accelerator Conference* **2** (1991) 1201 https://accelconf.web.cern.ch/accelconf/p91/PDF/PAC1991_1201.PDF.

[20] J.L. Sirvent, B. Dehning, J. Emery and A. Dieguez, *High dynamic range diamond detector readout system for the CRRN's beam wire scanners upgrade program*, Proceedings of *IBIC-2015*, Melbourne, Australia, September 13–17, 2015, https://accelconf.web.cern.ch/AccelConf/IBIC2015/papers/tupb053.pdf.

[21] S. Greco, A. Giglia, M. Malvezzi, S. Nannarone, S. DalZilio and M. Lazzarinoa, *Microfabricated wire scanner for photon beam characterization*, 2018 *JINST* **13** C03037.

[22] R.I. Cutler, D.L. Mohr, J.K. Whittaker and N.R. Yoder, *A High Resolution Wire Scanner Beam Profile Monitor with a MicroproceSSOR Data Acquisition System*, *IEEE Trans. Nucl. Sci.* **30** (1983) 2213.

[23] S. Igarashi, D. Arakawa, K. Koba, H. Sato, T. Toyama and M. Yoshii, *Flying wire beam profile monitors at the KEK PS main ring*, *Nucl. Instrum. Meth.* **A 482** (2002) 32.

[24] D. Bote, F. Salvat, A. Jablonski and C.J. Powell, *Cross sections for ionization of K, L and M shells of atoms by impact of electrons and positrons with energies up to 1 GeV: Analytical formulas*, *Atom. Data Nucl. Data Tabl.* **95** (2009) 871.

[25] R.M. Nazhmudinov, P. Karataev, A. Kubankin, K. Lekomtsev, A. Potylitsyn and A. Vukolov, *Experimental station with continuous electron beam for investigation of various mechanisms of EM radiation generation*, 2018 *JINST* **13** C06007.

[26] E.A. Heighway, K.J. Hohban and S.O. Schriber, *Electron beam current, profile and position monitor*, (1977), United States patent https://patents.google.com/patent/US4059763A/en.

[27] *Tables of Physical & Chemical Constants. 4.2.1 X-ray absorption edges, characteristic X-ray lines and fluorescence yields*, Kaye & Laby Online. Version 1.1 (2008), http://www.kayelaby.npl.co.uk.

[28] A.G. Afonin et al., *Characteristic X-ray radiation excited by 450 MeV/nucleon C +6 ions and 1.3 GeV protons in extracted and circulated beams of accelerator U70*, *Nucl. Instrum. Meth.* **B 355** (2015) 347.

[29] M. Andreyashkin et al., *Enhancement of the characteristic X-ray yield from oriented crystal irradiated by high-energy electrons*, *Nucl. Instrum. Meth.* **B 173** (2001) 142.

2018 JINST 13 P12012